Recent results from FOPI from the dynamics of heavy ion collisions to the (Anti)Kaon-nucleon potential

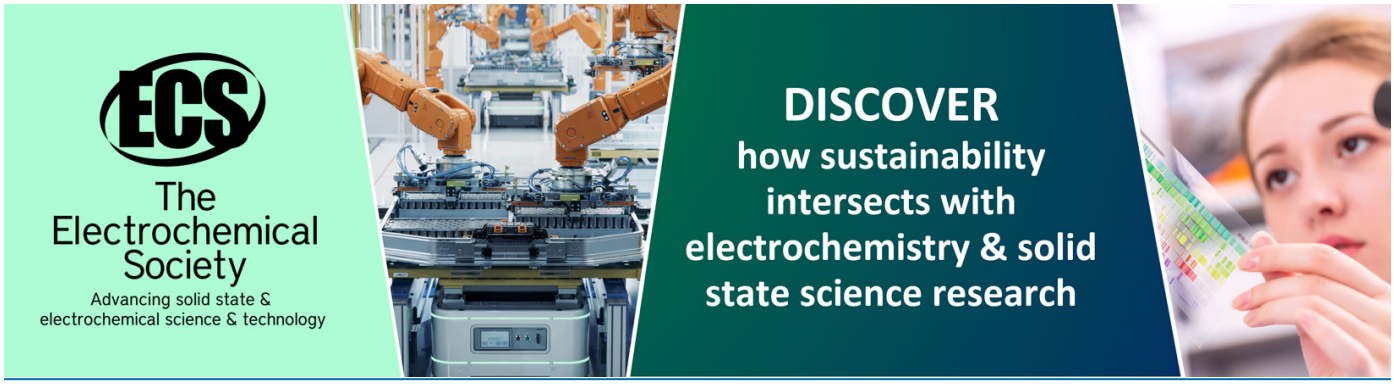

Journal of Physics: Conference Series **230** (2010) 012002 doi:10.1088/1742-6596/230/1/012002

Recent results from FOPI
From the dynamics of heavy ion collisions to the (Anti)Kaon-nucleon potential

Yvonne Leifels for the FOPI Collaboration
GSI Helmholtz Center for Heavy Ion Research, D-64291 Darmstadt, Germany
E-mail: Y.Leifels@gsi.de

Abstract. Strange particles allow to probe the properties of hot and dense baryonic matter. At incident energies close to the production threshold medium effects on the strange hadrons are magnified. New data obtained with the recently completed FOPI upgrade are presented for the system Ni+Ni at 1.91 AGeV and discussed in comparison to earlier findings.

1. Introduction

Modifications of hadron properties in dense baryonic matter are a current subject of intensive research in hadron physics. Various theoretical approaches [1, 2, 3] agree qualitatively in predicting, for example, modifications of masses and coupling constants for kaons and anti-kaons. Due to the density dependence of the KN($\overline{\text{K}}$N) potential, the K^- effective mass is expected to drop, whereas the mass of K^+ mesons is predicted to rise with increasing density of nuclear matter. Already two decades ago, Kaplan and Nelson [4] pointed out that due to additional attractive interactions with the surrounding nucleons a condensation of anti-kaons (K^-) may take place in a dense baryonic environment as encountered in the interior of neutron stars.

From general arguments one can conclude how the medium-modifications of the KN($\overline{\text{K}}$N) potentials influence particle production yields and phase space distributions. However, access to the depth of those potentials is only possible via microscopic transport codes modeling the dynamical evolution of heavy ion collisions.

At AGS energies clear evidence was found that the directed K^0 flow is opposite in sign to the flow of protons [5]. This experimental observation was explained by microscopic model calculation incorporating a repulsive KN potential [6]. Experimental data for charged kaons where less convincing and still lacking a consistent description [7]. At lower energies the sensitivity to the KN($\overline{\text{K}}$N) potential should be enhanced and several investigations by the KAOS, FOPI and lately HADES collaborations have been started at the SIS-18 accelerator at GSI.

The strength of the K^- nucleon potential might give rise to a new class of bound states [8, 9] with quite exotic properties. These bound states are called kaonic clusters and are being searched for in experiments using stopped K^- beams [10, 11] and pp reactions [12]. Due to the predicted large central densities and the large compression reached in the collision of heavy ions the production of kaonic clusters might be favored in such an environment [13]. Therefore a complementary program was started to look for bound multi baryonic strange states in heavy ion reactions [14].

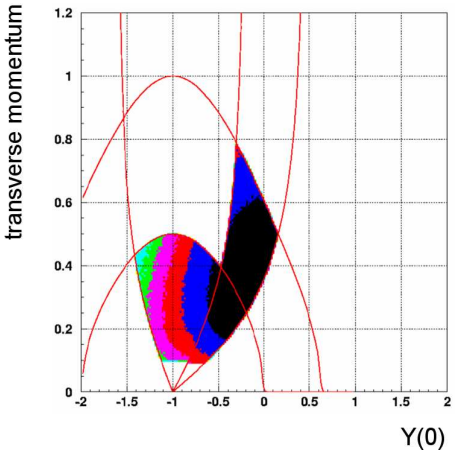

Figure 1. Acceptance for charged kaons making use of CDC - RPC and CDC - Plastic Barrel matches.

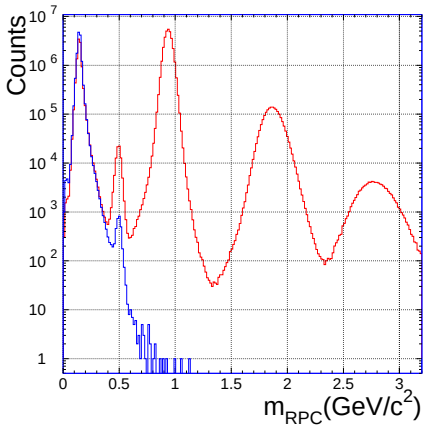

Figure 2. Reconstructed masses of positive (negative) charged particles using CDC–MRPC matches with a momentum cut of 1.0(0.8) GeV/c.

In the following new data obtained with the FOPI detector in 2008 at the SIS18 accelerator of GSI are shown for the reaction Ni+Ni at an incident energy of 1.91 AGeV together with older data from Al+Al collisions at the same energy elucidating some key aspects of strangeness physics in the threshold energy range.

2. Experiment: FOPI - Phase III

FOPI is a large acceptance detector system designed to measure charged particles emitted form heavy-ion collisions. It is installed at the SIS-18 accelerator at the GSI, Darmstadt (Germany). The modular structure allows to cover nearly the full solid angle in the laboratory frame. The core part of FOPI is a supra conducting solenoid with two drift chambers. The Central Drift Chamber CDC covering $30° < \Theta_{lab} < 140°$ and the forward drift chamber Helitron $7° < \Theta_{lab} < 30°$. Both drift chambers are augmented by time–of–flight–detectors for charge identification.

Apart from charged particles FOPI can measure neutral strange particles by their charged decay product ($K^0 \rightarrow \pi^+ + \pi^-$, branching ration BR = 69 %, $\Lambda \rightarrow \pi^- +$ p, BR =64 %, $\Phi \rightarrow K^+ + K^-$, BR = 49.1 %) as well as short lived strange resonances $\Sigma^{\pm *}$ and K^{0*}.

In order to improve the detection of charged kaons the FOPI detector was upgraded with a new time-of-flight barrel covering the polar angle range $35° < \Theta < 60°$ based on Multigap–Resistive–Plate–Chambers (MRPC) [15] in 2006. In the polar angle range $60° < \Theta < 140°$ a plastic scintillator barrel is used as a time–of–flight detector. The phase region in which charged kaons are thus identified in the FOPI Phase III setup is depicted in Fig. 1. Since then this detector was used in major data taking runs for which first result become available now. The performance in identifying the emitted particles is depicted for the reaction Ni+Ni at an incident energy of 1.91 AGeV in Fig. 2 where a mass spectrum is shown that is determined from the momentum reconstructed in the Central Drift Chamber (CDC) and the velocity measured in the MRPC barrel. The overall time resolution is 90 ps, in which the MRPC resolution is $\sigma_{tof,MRPC} = 65$ ps. This time resolution and the granularity of the detector are sufficient to separate positively (negatively) charged kaons with a signal-to-background ratio in excess of 10 when the maximum momentum is limited to 1.0 (0.8) GeV/c, respectively.

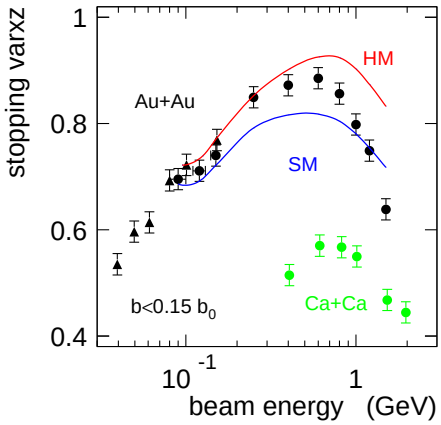

Figure 3. Stopping variable *varxz* as function of beam energy for central Au+Au and Ca+Ca collisions. The data for Au+Au collisions is a compilation of FOPI (filled circles) and INDRA (filled triangles) [34] results. The red and blue lines are prediction from the IQMD model [21] using a hard (HM) or a soft (SM) equation of state with momentum dependent interactions, respectively.

3. Dynamics of Heavy Ion collisions

After production the kaons are interacting with the surrounding matter. Some of these interactions are due to the respective KN or ($\overline{\text{K}}$N potentials. Negatively charged Kaons are additionally subject to strong absorption and positive kaons, despite their relatively long mean free path in a nuclear medium, are frequently rescattered. Hence, it is indispensable to measure phase space distributions of nucleons and light fragments to control the properties of the bulk matter and to constrain the input to microscopic transport models.

A relevant observable measuring the stopping in central collisions and the amount of energy redistributed from the primary longitudinal direction into the transverse direction is the ratio of the variances of the rapidity distributions in x–direction (*varx* transverse to the beam direction) and the rapidity distribution in z–direction (*varz* longitudinal). This observable *varxz* (or *vartl*) was introduced in [33]. The integrations for calculating the variances are limited to the range $|y_{z0}|, |y_{x0}| < 1$, where $|y_{z0}|, |y_{x0}|$ are scaled rapidities (i.e. $y_0 = y_{lab}/y_{cm,proj} - 1$). Other observables were introduced to characterise stopping (e.g. [31, 32]). Their common feature is that they assess stopping with respect to the initial conditions, whereas *varxz* refers to a completely stopped scenario (i.e. $varxz = 1$).

For the data points in Fig. 3 all measured charged particles have been added up to try to characterise the global system stopping in central collisions ($\approx 2\%$ of σ_{reac}). The excitation curve of *varxz* for Au+Au [33] was combined with data points from lower energies [34]. The observable *varxz* rises with energy and reaches a plateau between 0.4 and 0.6 AGeV, but obviously the colliding Au+Au system is not completely stopped, i.e. the rapidity distribution is more elongated in tranverse than in longitudinal direction. At energies beyond 0.8 AGeV *varxz* is rapidly dropping. The data points for the smaller Ca+Ca system are shown for comparison. Generally, they depict a similar behaviour with the slight shift of the maximum to higher energies but the elongation of the rapidity distributions in the beam direction is more pronounced for all investigated beam energies.

The Au+Au data are confronted with IQMD [21] predictions incorporating a hard (HM)

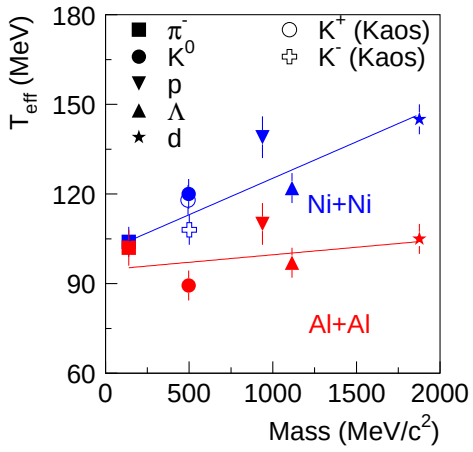

Figure 4. Inverse slope parameter T_{eff} as function of particle mass for Ni+Ni and Al + Al central collisions. Data points measured by the KAOS collaboration [36] are included where measured.

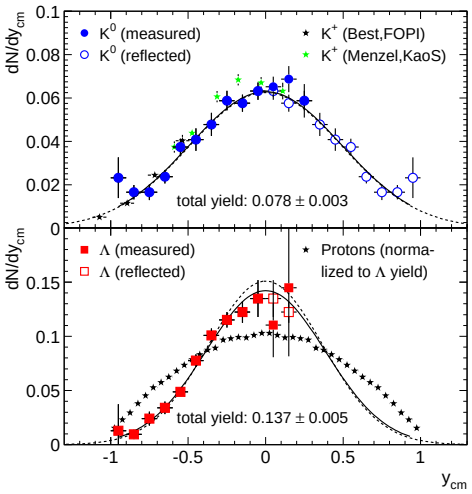

Figure 5. Rapidity density distributions for K^0 (full circles, upper panel) and Λ particles (filled squares, lower panel) in central Ni+Ni collisions at 1.93 AGeV. The open data points are reflected with respect to mid-rapidity. The (green and black) star symbols correspond to previously measured K^+ [36] (upper panel) and to protons (lower panel). The full line corresponds to a Gaussian fit, the dashed line is a prediction of a thermal model with radial flow [37].

and a soft (SM) equation of state with momentum dependent interaction. As can be seen in Fig. 3 *varxz* is sensitive to the mean-field EOS and opens up a possibility to observe EOS dependence also in central reactions. However, it is also clear that other interactions (i.e. collisions) influence the outcome of the calculations. The present parameterizations of IQMD are not able to reproduce the data at energies beyond 0.8 AGeV but a fair description with a hard equation of state is reached at lower energies.

The observed incomplete stopping in central collisions at SIS beam energies can be identified as partial transparency: This scenario is favoured by the observed system size dependence, and it was demonstrated explicitly by the so-called isospin tracing method combining the rapidity distributions of four collisions systems using ^{96}Zr and ^{96}Ru [35]. These results support the interpretation of central collisions at SIS energies in terms of two remnant counterflowing (not completely stopped) fluids and suggest that an equilibrium is not reached.

4. Strangeness production

The FOPI collaboration investigated the strangeness production for Al+Al (small size) and Ni+Ni (medium size) systems at $E_{beam} = 1.93$ AMeV. Two neutral strange particles, K^0 and Λ were reconstructed for about 20 % of the most central collisions of the total reaction cross

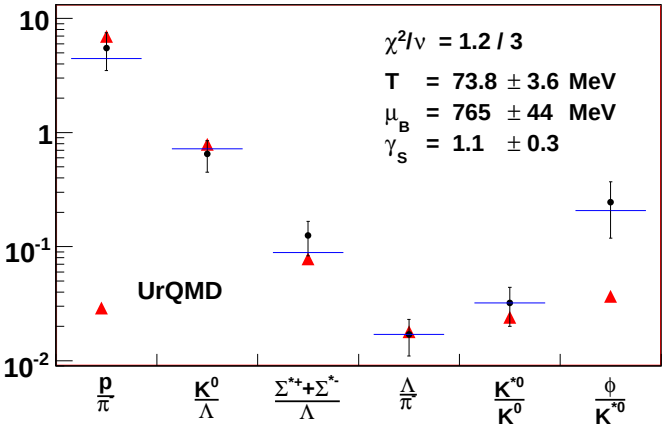

Figure 6. Independent particle ratios for central Al+Al [26] collisions with the results of thermal model fits and UrQMD predictions.

section [24]. The analysis of the phase space occupied by K^0s and Λs at freeze-out revealed that a thermal Boltzmann distribution with a single inverse slope parameter, T, is sufficient to describe the profiles of transverse mass distributions in subsequent rapidity bins. The inverse slope parameters T_{eff} at mid-rapidity for Ni+Ni and Al+Al collisions are shown in Fig. 4 together with the results for other particle species. For the heavier system T_{eff} is rising with particle mass which is commonly interpreted as flow. In a simplified picture the kinetic energy of a particle is the sum of a chaotic 'thermal' motion and flow therm which is linearly rising with particle mass. This is approximately the case for Ni+Ni collision, contrasting the smaller Al+Al system which does not show any significant flow. The less pronounced flow can be linked to the smaller system size and, therefore, smaller pressure build-up during the collision. The individual inverse slope parameters of the different particle species are not following strictly a linear trend: The appearent temperature of the Λ - Hyperons are significantly smaller than the one of protons with a similar mass, but clearly more systematic studies are needed to confirm this observation.

The rapidity density distribution along the beam axis of Λ's is significantly less elongated than the proton rapidity distribution (Fig. 5. Its shape is nearly gaussian and can be reproduced by a simple thermal model incorporating radial expansion [37]. The K^0 rapidity density distributions follows likewise the thermal model predictions. In contrast to the protons still keeping a trace of the initial state, the produced strange particles have lost the reminiscence of the entrance channel for the most part.

Φ mesons are reconstructed via their dominant decay channel $\Phi \rightarrow K^+ + K^-$ and yield have been extraced for central collisions of Al+Al and Ni+Ni at 1.9 AGeV. The strange resonances $\Sigma^{\pm *}(1385)$ and $K^{0*}(892)$ (Σ^* and K^* further on) also decay into charged particles which are accesibble to FOPI: $\Sigma^* \rightarrow \Lambda + \pi^{\pm}$ and $K^* \rightarrow K^+ + \pi^-$. The short lifetimes of those resonances ($c\tau = 5$ fm/c and 4 fm/c) leaves their decay vertices to close to the event vertex to be separated. Hence, their decay products cannot be distinguished from the other charged particles by a vertex cut. Despite the resulting huge background about 3100 ± 500 and 6100 ± 850 resonances were found with a significance of 9 and 10 [26], the invariant masses are in agreement with the values reported in literature. The efficiency corrections necessary to extract the particle yields are described e.g. in [26] or [43].

In total, 6 independent ratios of particle yields were constructed for central collisions of Al+Al at 1.91 AGeV beam energy. These ratios were compared to the statistical model predictions

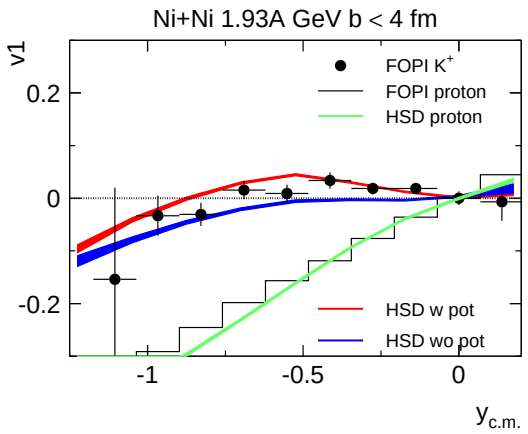

Figure 7. Results for directed flow v_1 of kaons in comparison to the flow of protons as a function of the center-of-mass rapidity $y_{c.m.}$. Solid lines are predictions using the HSD transport code.The v_1 - values are obtained within the acceptance of the CDC, for details see text.

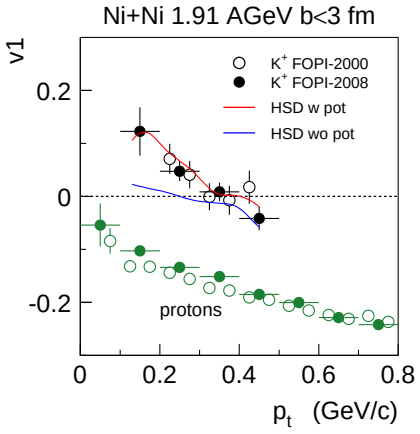

Figure 8. Directed flow v_1 of kaons as function of transverse momentum p_t in comparison to the flow of protons. Data from the new MRPC barrel (full circles) are compared to older results (filled circles) [16]. Solid lines are predictions of the HSD transport code with or without KN potential.

performed with the THERMUS code [38], as shown in Fig. 6. The calculations were done in the frame of a Grand Canonical ensemble for non-strange particles. Due to a necessity to constrain the strangeness number S at low beam energies, a Canonical ensemble was used for particles characterized by S $\neq$ 0 [39]. In general, a good fit–quality of the statistical model parameters Temperature T and baryo–chemical potential μ_B was obtained, expressed by $\chi^2/\nu = 0.3$ for Al+Al. The best fits were found for T of about 74 MeV and μ_B of about 780 MeV respectively. These values match the systematics of T and μ_B extracted at other beam energies and systems [40]. In case of Al+Al it was possible to fit in addition the strangeness undersaturation factor γ_S, being non-equal to unity in case of non-equilibration of the yield of particles containing strange quarks [41]. However, it was found to be consistent with unity within the experimental errors. These results demonstrate that the statistical model with two (three) free fit parameters of T, μ_B (and γ_S) is capable of reproducing the experimental yield ratios at 1.9 AGeV, despite the observation that the underlying assumption of a complete equilibration is not supported by the experimental rapidity profiles of nuclear bulk matter.

Similar observations have been made in Ni+Ni collisions at 1.9 AGeV: All particle ratios are described within a thermal model yielding similar parameters [44]. There is only one prominent exception the η/π ratio, a fact which was already reported in the literature (e.g. [42]).

It is interesting to note that the measured particle ratios in central Al+Al collisions are reasonably well described by the microscopic transport code UrQMD [45]. UrQMD results were found to be in agreement not only with experimental data, but also with the predictions of the statistical model except for the Φ/K^* yield ratio. It is known, however, that the production yield of Φ mesons in UrQMD too low in this energy range [46]. Apart from the Φ meson the qualitity of description is equally good for both models. To draw further conclusions one needs more systematic studies on heavier collision systems and different energies.

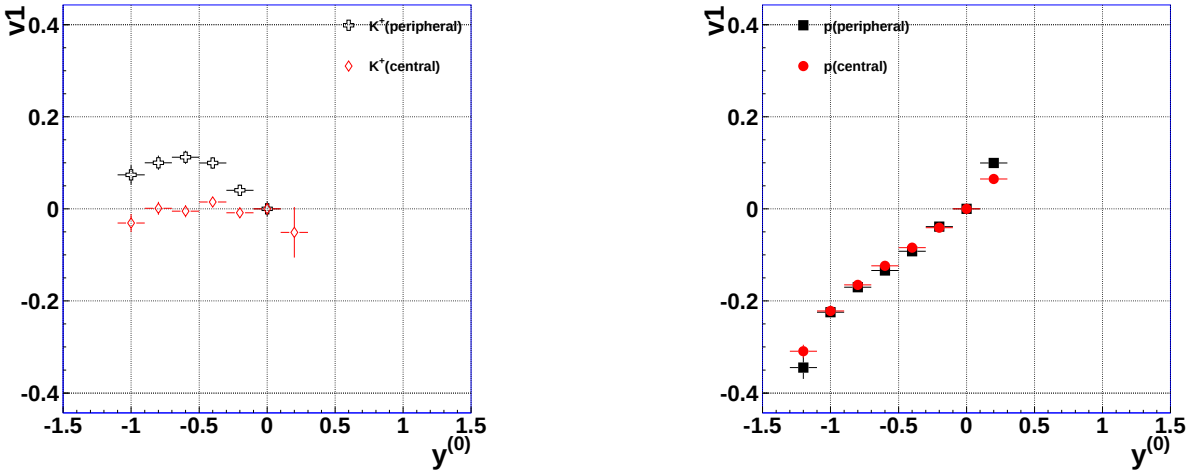

Figure 9. Sideflow of kaons and protons in the reaction Ni+Ni at an incident energy of 1.91 AGeV as function of normalized rapidity $y(0) = y/y_{cm,proj}1$. The first fourier coefficients v_1 are plotted for two different centrality bins for kaons (left panel) and protons (right panel). Black data points are obtained for peripheral collisions corresponding to a mean impact parameter of 6 ± 1 fm, the red ones for central collisions with a geometrical impact parameter b < 3 fm. The v_1–values are obtained within the acceptance of the CDC, for details see text.

5. Kaon flow

The excellent kaon identification capabilities of the MRPC barrel allows to perform differential flow analysis of these rare particles and thus to continue the effort to determine the in-medium potential for kaons and anti-kaons [16].

In Fig. 7 the first fourier coefficients v_1 [18] measured in central Ni+Ni collisions at 1.91 AGeV are plotted as function of the normalized rapidity for positive kaons and protons together with predictions of the HSD model [47] with and without a KN nucleon potential. The direction of the reaction plane was determined by the transverse momentum method [19] making use of particles detected in the forward wall of FOPI only in order to avoid autocorrelations. The data are corrected for the finite reaction plane resolution employing the Ollitrault formalism [20]. For better comparability with different reaction plane reconstruction methods the v_1 data were shifted such that the mean $v_1$value at midrapidity is antisymmetric. In order to compare to the data shown in Fig. 7 model calculations have to take into account the acceptance of the detector, that is limited for this detailed analysis to the acceptance of the CDC covering a polar angle range of $26° < \Theta_{lab} < 120°$. For kaons additional constraints have to be put on the momenta necessary to obtain sufficient particle identification in the data. In the polar angular range from $30.5° < \Theta_{lab} < 52°$ (MRPC acceptance) kaons are included up to a momentum of 1.0 GeV/c, in the range $53° < \Theta_{lab} < 120°$ (plastic barrel acceptance) the laboratory momentum is limited to 0.5 GeV/c. The angular limits correspond to the so called shifted target geometry, where the target was placed 40 cm upstream of its nominal position in the FOPI apparatus.

The microscopic model results agree reasonably well with the experimental data for kaons and protons, however, the sensitivity of this obervable to the in-medium KN potentials is rather small. The repulsive KN potential pushes the kaons away from the bulk matter, but the effect is moderate. The picture changes if one includes the transverse direction and switches to v_1 as a function of rapidity *and* transverse momentum. In Fig. 8 experimental data measured in 2000 [16] is shown together with the new results confirming the old findings. One observes a strong p_t dependence for kaons. The fourier coefficient v_1 is changing sign. For low p_t the kaon flow

signal is opposite to the one of the protons which may signal the influence of the KN potential being more relevant for small transverse momenta. At larger transverse momenta the directed flow of kaons tends to be negative like the one of the protons. The HSD transport code is only able to reproduce this observation when a repulsive KN potential is considered. A potential of $U_{pot} = 20MeV$ at normal nuclear matter density is describing the data. This is consistent with results from pion induced reactions measured by the FOPI collaboration [17].

Another effect sensitive to the KN potential is observed in the centrality dependence of v_1 (Fig. 9). The centrality selection was chosen such that for both centrality bins the proton flow is still approximately the same within the detector acceptance. The event samples differ by the amount of stopping, the maximum density reached in the collision zone and the size of the cold spectator matter. The latter manifests itself at rather low transverse momenta which are not accessible in the chosen acceptance of this analysis. While the kaon data in the central event sample confirm quantitatively our earlier findings as shown before, the large sideflow in the most peripheral data sample is suprising: At a normalized rapidity of y(0)$\approx$ 0.5 the antiflow of the kaons has the same magnitude as the flow of the protons. Tentatively, this effect can be attributed to the strong momentum dependence of the kaon potential. This hypothesis awaits its confirmation/rejection by transport model calculations.

The available data sample also allows the reconstruction of the K^- flow. However, this analysis is much more difficult due to the very low yield of K^- that is at the 3 % level of K^+ production. The analysis is in progress.

6. Summary

The observable *varxz* characterizes stopping (i.e. the redistribution of momentum from the longitudinal into the transverse direction) in heavy ion collisions with respect to a fully stopped system by correlating the variance of the rapiditity distribution in the transverse direction to the one in the longitudinal direction. The *varxz* reaches a maximum between 0.6 and 0.8 AGeV and drops rapidly at higher energies. This observation was identified as increasing 'partial transparency' of two counterflowing fluids never reaching global equilibration. Nevertheless, yield ratios of nucleons and produced particles can be described by thermal model fits.

New data have been presented making use of the FOPI phase III setup at GSI elucidating the properties of strange particle in dense baryonic matter. For the first time a strong antiflow component for K^+ is seen for peripheral Ni+Ni reactions at 1.91 AGeV. pointing to a strong momentum dependence of the Kaon-Nucleus potential. More data are available from the 2009 measurement campaign of FOPI where more than 10^8 events were recorded for the reactions Ni+Pb at an incident energies of 1.91 AGeV and Ru+Ru at 1.65 AGeV opening new possibilities to study hadronic states in the hadronic environment of a heavy-ion collision.

Acknowledgments
This work was supported by the German BMBF under Contract No. 06HD190I, by the Korea Science and Engineering Foundation (KOSEF) under Grant No. F01-2006- 000-10035-0, by the mutual agreement between GSI and IN2P3/CEA, by the Hungarian OTKA under Grant No. 47168, within the Framework of the WTZ program (Project RUS 02/021), by DAAD (PPP D/03/44611), by DFG (Projekt 446-KOR-113/76/04) and by the EU, 6th Framework Program, Integrated Infrastructure: Strongly Interacting Matter (Hadron Physics), Contract No. RII3-CT-2004-506078.

References

[1] Brown G E et al. 1994 *Nucl. Phys.* A **567** 937
[2] Weise W *Nucl. Phys.* A **610** 35c
[3] Li G Q et al. 1997 *Nucl. Phys.* A **625** 372

[4] Kaplan D B and Nelson A E 1986 *Phys. Lett.* B **175** 57
[5] Chung P et al. [EOS collaboration] 2000 *Phys. Rev. Lett* **85** 340-943
[6] Pal S, Ko C M, Li Z, Bin Z 2000 *Phys. Rev.* C **62** 061903
[7] Pinkenburg C et al. [EOS collaboration] 2002 *Nucl. Phys.* A **698** 495-498
[8] Akaishi Y and Yamazaki T 2002 *Phys. Rev.* C **65** 044005
[9] Yamazaki T, Doté A, Akaishi Y 2004 *Phys. Lett.* B **587** 167
[10] Agnello M et al. 2005 *Phys. Rev. Lett.* **94** 212303
[11] Suzuki T et al. [E549 collaboration] 2008 *Mod.Phys.Lett.* A **23** 2520
[12] Yamazaki T et al. (*Prepint*) arXiv:0810.5182
[13] Yamazaki T et al. 2004 *Nucl. Phys.* A **738** 168
[14] Herrmann N [FOPI collaboration] 2005 *Proceedings of the EXA05 conference, Osterreichische Akademie der Wissenschaften* 73
[15] Schüttauf A et al. 2009 *Nucl. Instr. Meth.* A **602** 679
[16] Crochet P et al. [FOPI collaboration] 2000 *Phys. Lett.* B **486** 6
[17] Benabderrahmane M L et al. [FOPI collaboration] 2009 *Phys. Rev. Lett.* **102** 182501
[18] Voloshin S A and Zhang Y Z 1996 *Z. Phys.* C **70** 665
[19] Danielewicz P and Odyniec G 1985 *Phys. Lett.* B **157** 146
[20] Ollitraut J Y 1997 (*Preprint* nucl-ex/9711003)
[21] Hartnack C et al. 1996 *Eur. Phys. J.* A **1** 151
[22] Ritman J et al. [FOPI collaboration] 1995 *Z. Phys.* A **352** 355
[23] Herrmann N, Wessels J P, Wienold T 1999 *Ann. Rev. Nucl. Part. Sci.* **49** 581
[24] Merschmeyer M et al. [FOPI collaboration] 2007 *Phys. Rev.* C **76** 02490
[25] Lopez X et al. [FOPI Collaboration] 2007 *Phys. Rev.* C **76** 052203
[26] Lopez X et al. [FOPI Collaboration] 2008 *J. Phys.* G **35** 044020
[27] Herrmann N [FOPI Collaboration] 2009 *Prog. Part. Nucl. Phys.* **62** 445
[28] Braun O et al. 1977 *Nucl. Phys.* B **124** 45
[29] Pigeot C et al. 1985 *Nucl. Phys.* B **249** 172
[30] Siebert R et al. 1994 *Nucl. Phys.* A **567** 819
[31] Videbaek F and Hansen O 1995 *Phys. Rev.* C **52** 2684
[32] Ströbele H 2009 *Preprint* nucl-ex:0908.2777
[33] Reisdorf W et al. [FOPI Collaboration] 2004 *Phys. Rev. Lett.* **92** 232301
[34] Andronic A, Lukasik J, Reisdorf W, Trautmann W 2006 *Eur. Phys. J.* A**30** 31
[35] Rami F et al. [FOPI Collaboration] 2000 *Phys. Rev. Lett.* **84** 1120; Hong B, et al. [FOPI Collaboration] 2002 *Phys. Rev.* C **66** 034901
[36] Menzel M et al. [KAOS Collaboratoin] 2000 *Phys. Lett.* B **495** 26
[37] Siemens P J and Rasmussen J 0 1979 *Phys. Rev. Lett.* **42** 880
[38] Wheaton S, Cleymans J, Hauer M 2004 *Preprint* hep-ph/0407174
[39] Braun-Munzinger P, Redlich K, Stachel J 2004 in Quark-Gluon Plasma 3, World Scientific Publishing, Singapore
[40] Braun-Munzinger P, Wambach J 2009 *Rev. Mod. Phys.* **81** 1031
[41] Becattini R et al. 2001 *Phys. Rev.* C **64** 024901
[42] Averbeck R, Holzmann R, Metag V, Simon R S *Phys. Rev* C **67** 024903
[43] Mangiarotti A 2003 *Nucl. Phys.* **A 714** 89
[44] Piasecki K 2009 Proceeding to the Bormio winter workshop on nuclar physics
[45] Bass S et al. 1998 *Prog. Part. Nucl. Phys.* **41** 225-370
[46] Bleicher M 2009 *private communication*
[47] Cassing W, Tolos L, Bratkovskaya E, Ramos A 2003 *Nucl. Phys.* **A 727** 59